Thermochimica Acta 491 (2009) 29–34

Contents lists available at ScienceDirect

Thermochimica Acta

journal homepage: www.elsevier.com/locate/tca

Liquid phase vapor pressure measurement and thermodynamics assessment of the Hg–In binary system

Wojcieh Gierlotka[a,b,*], Piotr Jarosz[a], Sinn-wen Chen[b]

[a] Non-Ferrous Metals Department, AGH University of Science and Technology, Mickiewicza 30, 30-059 Krakow, Poland
[b] Department of Chemical Engineering, National Tsing Hua University, #101, Sec. 2, Kuang-Fu Rd., Hsin-Chu 300, Taiwan

ARTICLE INFO

Article history:
Received 24 October 2008
Received in revised form 23 February 2009
Accepted 24 February 2009
Available online 9 March 2009

Keywords:
Phase diagrams
Thermodynamic properties
Thermodynamic modeling

ABSTRACT

The vapor pressure of mercury over molten Hg–In alloys was measured, and the results were used for the activity determination. Thermodynamics assessment of the Hg–In binary system was conducted using the Calphad approach based on the experimental results determined in this study as well as those found in the literature. The Hg–In phase diagram was calculated using assessed thermodynamic models. It was found that the calculated thermodynamic properties and phase diagram are in good agreement with the experimental data.

1. Introduction

Hg–In alloys could be a part of superconductor or semiconductor multicomponent systems [1–3]. The phase diagram and thermodynamic properties of Hg–In binary system are fundamentally important for applications, and have been investigated previously [4–28]. It is known that the mercury is toxic and has high vapor pressure. In this study the vapor pressure of Hg–In alloys was measured using static method, and the obtained results were used for the activity determination of mercury. Thermodynamic remodeling of the Hg–In system is then conducted based on the Calphad approach [29] using the experimental data obtained in this study as well as those taken from the literature [4–28].

2. Literature information

The first diagram of the Hg–In binary system has been published by Ito et al. [4]. The indium rich corner has been examined by Spicer and Banick [5] and Tyzack and Raynor [6]. Very wide description of phase diagram is in Kozin's [7] book about amalgams systems. Kozin's proposition of phase diagram includes five intermetallic compounds: Hg_6In, Hg_4In, HgIn, $HgIn_2$ and $HgIn_{11}$; however, later study (Mahy and Gissen [8]) showed that Hg_6In and Hg_4In are FCO phase. Another Kozin's [9] work was experimental. He studied phase diagram using thermal analysis. Eggert [10] in his work made review of liquidus curve of Hg–In binary system, after that Jangg [11] and Chiarenzelli and Brown [12] described phase diagram based on thermal analysis. The phase FCC_A1 has been investigated by Coels et al. [13] who described phase boundaries of this phase by superconductivity measurement. Finally, Morawietz [14] correctly determined phase diagram with homogeneity region around HgIn intermetallic compound. The last change of the phase diagram was made by Claeson and Merriam [15], who discovered compound $HgIn_2$ which forms from HgIn and FCC_A1 phases at 218 K. The latest published version of phase diagram is proposition made by Okamoto which has been adopted by Massalski in "Binary Alloy Phase Diagrams" [16]. Crystal structure for composition up to 55 at.% of indium at temperatures between 12 and 183 K has been examined by Heller and Musgrave [17].

Thermodynamic properties of the liquid phase were investigated by many authors. The first work was done by Richards and Wilson [18] who used EMF measurement. Butler [19] used also EMF method for describing activity coefficient of indium in liquid Hg–In at 298 K. Activities of mercury between 557 and 696 K have been studied by Predel and Rothacker [26]. Activities of elements in liquid phases at 298 K were examined also by Okajima and Sako [27] and Damelincourt et al. [28].

Heat of mixing of liquid Hg–In alloys was determined by Kleppa and Kaplan [20] at 433 K. In other works, Kleppa [21] and also Witting and Scheidt [22] measured enthalpy of mixing of the liquid phase at 313, 373, 423 and 473 K. Partial enthalpies of mixing at 416 and 426 K were measured by Bros [23]. Enthalpies of formation of solid alloys have been investigated by Singh and Misra [24] who studied full range of composition at 192 K. Generally, one can say that experimental information about the liquid phase agreed with one other and show negative deviation from the Raoult Law.

* Corresponding author at: Non-Ferrous Metals Department, AGH University of Science and Technology, Mickiewicza 30, 30-059 Krakow, Poland.
E-mail address: gilu@uci.agh.edu.pl (W. Gierlotka).

0040-6031/$ – see front matter © 2009 Elsevier B.V. All rights reserved.
doi:10.1016/j.tca.2009.02.020

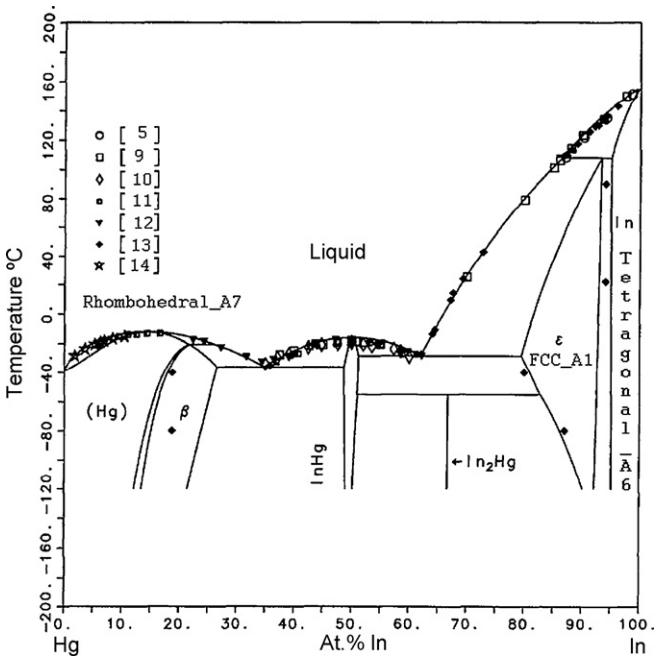

Fig. 1. The Hg–In binary system published by Hansen [41].

Activities of components of the solid phase have been studied by EMF method by Sunden [25] and Kozin and Tananaeva [9]. The previous calculation of the Hg–In binary system was done by Hansen [41]. As we mentioned he used liquid phase as a reference state of all phases except for HgIn IMC which can make some expansion to high-order systems difficult. Published by Hansen [41] phase diagram is shown in Fig. 1.

In this work the following phases are considered: *Liquid*, *Rhombohedral_A7*, *FCO*, *FCC_A1*, *Tetragonal_A6*, *HgIn* and $HgIn_2$. Description of the crystal structure is given in Table 1. The system exhibits also five invariant reactions at 381, 253, 243, 236 and 218 K. The liquidus line is below 273 K for concentration up to 0.65 mole fraction of In.

Table 1
Crystal structures of the phases in Hg–In system [16].

Phase	Pearson system	Space group	Strukturbericht designation	Prototype
Rhombohedral (Hg)	*hR1*	$R\bar{3}m$	A10	αHg
FCO	*oF8*	*Fddd*	...	γPu
HgIn	*hR2*	$R\bar{3}m$	$L1_1$	CuPt
FCC	*cF4*	$Fm\bar{3}m$	A1	Cu
Tetragonal	*tI2*	*I4/mmm*	A6	In

For higher content of indium liquidus line increases to the melting point of pure indium. The system includes also two intermetallic compounds: HgIn and $HgIn_2$.

3. Experimental procedures

The activities of mercury in Hg–In alloys were determined using the vapor pressure measurement method. Pure mercury (99.99%) obtained from Polish Chemical Reagents was additionally distillated in vacuum. Indium of 99.99% purity was also obtained from Polish Chemical Reagents. Samples of alloys were prepared separately by weighing appropriate amounts of metals and melting them in silica chamber at temperature so high that the Hg vapor pressure reached about 0.9 bar. Under these conditions the system has been kept for 3–4 h and then cooled. If the pressure in reactor after cooling was greater than 1.5E − 2 hPa, the reactor had been opened and evacuated and the whole procedure has been repeated. Then, samples were used in further measurements of the vapor pressure over liquid phase.

The scheme of the apparatus is shown in Fig. 2. The measurements of pressure of metal vapors consist in the use of a glass pressure gauge. This technique, developed years ago by Gibson [30], and used for determination of dissociation pressure of cupric bromide by Jackson [31], has been also successfully applied to the determination of the parameters of ZnO reduction process [32,33], and vapor pressure over Hg–Tl alloy [34]. Consequently, it can be also applied to the vapor pressure determination of mercury over liquid Hg–In alloy.

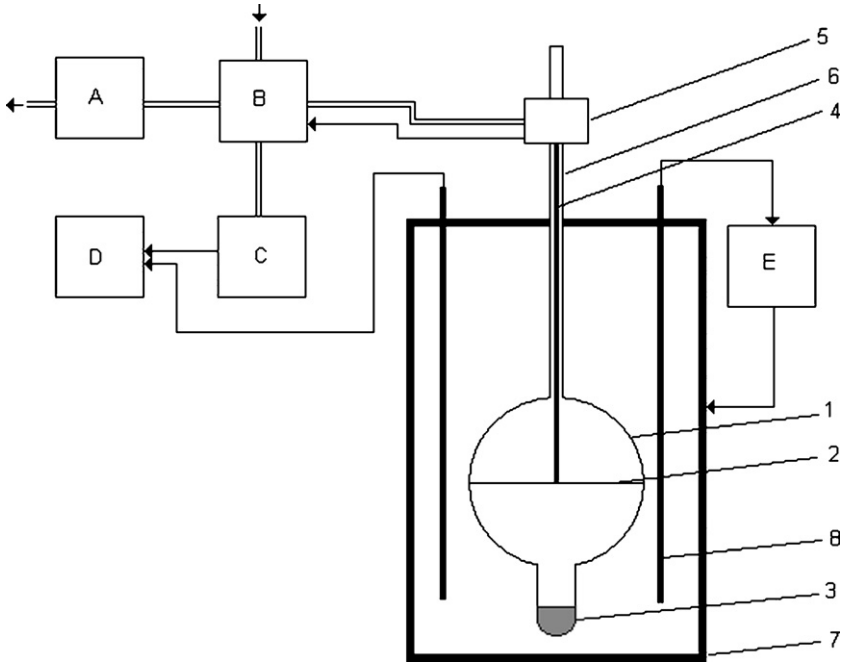

Fig. 2. Experimental arrangement. 1: silica vessel, 2: silica membrane, 3: vaporization chamber, 4: silica rod, 5: transoptor, 6: silica tube, 7: furnace, 8: thermocouple, A: vacuum pump, B: pressure switch, C: pressure measurement device, D: computer, E: temperature regulator.

Table 2
Description of vapor pressure [hPa] over liquid Hg–In system.

X_{Hg}	a	b	T [K] measurement range
0.0314	−66,733.2	122.9754	600–945
0.0506	−66,604.3	127.443	520–890
0.06945	−66,250	130.147	565–910
0.1002	−65,808	133.1025	516–850
0.2008	−64,490	138.764	523–730
0.3002	−63,307.2	142.087	470–695
0.4001	−62,348.6	144.497	465–715
0.4502	−61,987.5	145.607	460–670
0.5001	−61,659.7	146.5915	460–690
0.5501	−61,172.5	147.2	480–680
0.6	−60,801.2	147.856	480–670
0.6989	−60,252.2	149.1365	470–670
0.8006	−59,853.2	150.251	470–660
0.8249	−59,777.2	150.508	480–640
0.85	−59,711.2	150.758	460–620
0.875	−59,654.2	150.999	460–625
0.8998	−59,607.5	151.312	470–620
1	−59,521.2	152.113	Ref. [35]

The main part of the apparatus consists of the silica vessel (1) which is divided into two parts by the silica membrane (2). A piece of prepared earlier Hg–In alloy (or pure mercury) of approximately 3 g has been placed in the vaporization chamber (3) which was evacuated and sealed under vacuum. In the upper part of the vessel a thin rod of silica was placed vertically on the membrane (4) in such a way that its upper part goes through the slit of transoptor (5). The rotary pump was connected with the upper part of the vessel through the silica tube (6). The vessel has been immersed in the resistant furnace (7). Additionally, a thick-walled iron crucible (8) was placed in the furnace to stabilize its thermal field. The accuracy of temperature has been less than 2 K, accuracy of measured pressure 1.5E − 2 hPa and accuracy of composition less than 0.001 mole fraction. The accuracy was limited by temperature and pressure measurement systems and by the balance used for sample preparation.

If temperature increases, the pressure over liquid alloy also increases. In this case, silica membrane (2) deflect and the rod (4) moves up, what changes mode of transoptor (5). Upon new mode of transoptor the pressure over membrane (2) increases till the pressures over and under membrane are equal to each other. Consequently, the silica rod (4) moves down and changes mode of transoptor (5) to neutral state. Opposite way of work was used when temperature of liquid alloy decreased, which means that the silica rod (4) moves down and changed mode of transoptor to the state when rotary pump was working. The pressure of a gas over silica membrane (2) was measured by electronic device and registered by computer.

4. Experimental results and discussion

For constant alloy composition the vapor pressure of Mercury over liquid phase, can be described by Eq. (1):

$$RT \ln P_{Hg} = a + bT \tag{1}$$

where R: gas constant [J/(mol K)], P: pressure [hPa], T: absolute temperature [K], a and b: coefficients.

The pressure of indium is negligible at experiment temperatures and equal 4.07E − 6 hPa at 900 K [9]. The temperature range of experiment was depend on composition of sample and varied between 460 and 940 K.

The result of experiment is shown in Table 2, where one can find set of coefficients for Eq. (1) obtained on the base of vapor pressure measurement over 17 samples. In the same table, description of the pressure of pure Hg vapor [35] is also shown. Values of a and b coefficients were obtained by the Statgraphics software [36].

The activity of Hg can be determined from the relation:

$$a_{Hg} = \frac{P_{Hg}}{P^0_{Hg}} \tag{2}$$

where a_{Hg}: activity of mercury, P_{Hg}: vapor pressure of mercury over liquid alloy, P^0_{Hg}: vapor pressure of mercury over pure mercury.

For further calculation it is more convenient to rewrite Eq. (1):

$$\ln P_{Hg} = \frac{a'}{T} + b' \tag{3}$$

where $a' = a/R$ and $b' = b/R$ and express activity in the form:

$$\ln\ a_{Hg} = \ln P_{Hg} - \ln P^0_{Hg} = \frac{a' - a^0}{T} + (b' - b^0) \tag{4}$$

and from commonly known equation, partial Gibbs energy of mercury is given by

$$\Delta\bar{G}_{Hg} = RT \ln a_{Hg} = R(a' - a^0) + \frac{R}{T}(b' - b^0) \tag{5}$$

The partial heat of mixing and partial entropy of mercury can be derived as well

$$\Delta\bar{H}_{Hg} = -RT^2 \frac{\partial \ln\ a_{Hg}}{\partial T} = R(a' - a^0) \tag{6}$$

$$\Delta\bar{S}_{Hg} = \frac{\Delta\bar{H}_{Hg} - \Delta\bar{G}_{Hg}}{T} = -R(b' - b^0) \tag{7}$$

As one can see it is very easy to calculate from Eqs. (5)–(7) thermodynamic function of the liquid phase; however, for full thermodynamic description of binary alloys its better to use more universal tool such a Calphad [29] method and Thermo-Calc [37] software.

5. Thermodynamic assessment and phase diagram calculation

The optimization of binary Hg–In system has been published previously [41]; however, taking into account new experimental information obtained in this work and reference states used by Hansen in his work (he used liquid as reference state for all phases) we decided to make optimization of this system again. Calphad [29] method is a very powerful tool which can be also used for systems in which the range of temperature includes values lower than 298 K [38].

Several thermodynamic models were used for the description of phases in Hg–In binary system:

5.1. Substitutional solution

The Gibbs energies of pure elements with respect to temperature ${}^0G_i(T) = G_i(T) - H_i^{SER}$ are represented by Eq. (1):

$${}^0G_i(T) = a + bT + cT\ \ln(T) + dT^2 + eT^{-1} + fT^3 + iT^4 + jT^7 + kT^{-9} \tag{8}$$

The ${}^0G_i(T)$ data are referred to the constant enthalpy value of the standard element reference H_i^{SER} at 298.15 K and 1 bar as recommended by Scientific Group Thermodata Europe (SGTE) [42]. The accepted reference states are: Liquid (Hg) and Tetragonal_A6 (In). The ${}^0G_i(T)$ expression may be given for several temperature ranges, where the coefficients a–f and i–k have different values. The ${}^0G_i(T)$ functions are taken from SGTE Unary (Pure elements) TDB v.4 [42]. The SGTE Unary database is defined from 298.15; however for this work we extrapolated Gibbs energy down to 200 K. The same trick was used during previous optimization by Hansen [41] and Gierlotka et al. [38].

Solid and liquid solution phases (*Liquid*, *Rhombohedral_A7*, *FCO*, *FCC_A1*, *Tetragonal_A10*) are described by the substitutional solution model [39]:

$$G_m(T) = \sum_i x_i^0 G_i(T) + RT\sum_i x_i \ln(x_i) + \sum_i \sum_{j>i} x_i x_j \left(\sum_\nu {}^\nu L_{ij}(x_i - x_j)^\nu \right) \quad (9)$$

where the $\sum_i \sum_{j>i} x_i x_j \left(\sum_\nu {}^\nu L_{ij}(x_i - x_j)^\nu \right)$ part is the Redlich–Kister polynomial describing excess Gibbs energy.

5.2. Two-sublattice model

The HgIn phase is formed in $L1_1$ structure with CuPt prototype. A description of the Gibbs energy of this phase is a two-sublattice model, $(Hg,In)_{0.5}:(Hg,In)_{0.5}$ [40]:

$$\begin{aligned} G_m^{HgIn}(T) = {} & y^I_{Hg} y^{II}_{Hg} {}^\circ G^{HgIn}_{Hg:Hg} + y^I_{Hg} y^{II}_{In} {}^\circ G^{HgIn}_{Hg:In} + y^I_{In} Y^{II}_{Hg} {}^\circ G^{HgIn}_{In:Hg} \\ & + y^I_{In} y^{II}_{In} {}^\circ G^{HgIn}_{In:In} + 0.5RT(y^I_{Hg} \ln y^I_{Hg} + y^I_{In} \ln y^I_{In}) \\ & + 0.5RT(y^{II}_{In} \ln y^{II}_{In} + y^{II}_{Hg} \ln y^{II}_{Hg}) + {}^{xs}G_m^{HgIn} \end{aligned} \quad (10)$$

where ${}^{xs}G_m^{HgIn}$ represents excess Gibbs energy:

$$\begin{aligned} {}^{xs}G_m^{HgIn} = {} & y^I_{Hg} y^I_{In} y^{II}_{Hg} L^{HgIn}_{Hg,In:Hg} + y^I_{Hg} y^I_{In} y^{II}_{In} L^{HgIn}_{Hg,In:In} + y^I_{Hg} y^{II}_{In} y^{II}_{Hg} L^{HgIn}_{Hg:In,Hg} \\ & + y^I_{In} y^{II}_{In} y^{II}_{Hg} L^{HgIn}_{In:In,Hg} + y^I_{In} y^I_{Hg} y^{II}_{In} y^{II}_{Hg} L^{HgIn}_{In,Hg:In,Hg} \end{aligned} \quad (11)$$

in which y_i^N denotes the site fraction of element i on sublattice N, symbol ":" indicates separation of elements on the different sublattices, and "," indicates separation of elements on the same sublattice.

5.3. Line compound model—$HgIn_2$

Stoichiometric compound $HgIn_2$ is described as the line compound using the following equation:

$$G_m^{HgIn}(T) = a + bT + 0.667GHSERIN + 0.333GHSERHG \quad (12)$$

where *GHSERIN* and *GHSERHG* are Gibbs energies of In in Tetragonal_A10 and Hg in liquid phases, respectively.

6. Calculated results and discussion

The thermodynamic parameters for all phases in the system were optimized by the Calphad [29] method using Thermo-Calc [37] software. The optimization was carried out in agreement with Schmid-Fetzer et al. [43] guideline. For this optimization, thermochemical data for the liquid phase, invariant reactions and liquidus/solidus information were used. To each piece of the selected information a certain weight was given by personal judgment. The optimization was carried out step by step. At first, optimization of the liquid phase was performed. Next, solid phases were assessed. Intermetallic compound HgIn was treated as line compound at first; however after initial optimization the description of this phase has been changed to two-sublattice compound energy model.

Finally all parameters were evaluated together to yield the best description of the system. The calculated interaction parameters are shown in Table 3.

Calculated thermodynamic properties of liquid phase are shown in Figs. 3–5. Fig. 3 shows calculated activity of mercury and indium compared with the experimental results of Damelincourt et al. [28], Sunden [25] and Predel and Rothacker [26] and this work. As can be seen from that figure, modeled activities of components show negative deviation from Raoult's Law and very good agreement with experimental data at very wide temperature range 298–696 K. Fig. 4 shows calculated at 500 K Gibbs energy of mixing and chemical potentials of mercury and indium superimposed with experimental information obtained in this work. Calculated heat of mixing super-

Table 3
Gibbs free energies of Hg–In system.

Phase	Parameters
Liquid	$L0 = -9691.195$
Rhombohedral_A10	$G_{In}^{Rhombohedral\_A10} = GHSERIN + 800$
	${}^0L_{HgIn}^{Rhombohedral\_A10} = -6038.819$
	${}^1L_{HgIn}^{Rhombohedral\_A10} = -6682.800$
FCO	$G_{Hg}^{FCO} = GHSERHG + 4258.238$
	$G_{In}^{FCO} = GHSERIN + 900$
	${}^0L_{HgIn}^{FCO} = -12993.501 + 132.436T$
	${}^1L_{HgIn}^{FCO} = -83669.322$
HgIn	$G_{Hg:Hg}^{HgIn} = GHSERHG + 5439.268 - 11.736T$
	$G_{In:In}^{HgIn} = GFCCIN*$
	$G_{Hg:In}^{HgIn} = 0.5GHSERIN + 0.5GHSERHG - 4786.312 + 6.422T$
	$G_{In:Hg}^{HgIn} = 0$
	$L_{Hg,In:Hg}^{HgIn} = -92.8785$
	$L_{Hg:In,Hg}^{HgIn} = -2154.2429$
	$L_{In:In,Hg}^{HgIn} = -1580.8171$
	$L_{Hg,In:In}^{HgIn} = 1746.7951$
$HgIn_2$	$G_{Hg:In}^{HgIn_2} =$ $0.333GHSERHG + 0.667GHSERIN - 5000 + 10.958 * T$
FCC_A1	$G_{Hg}^{FCC\_A1} = GHSERHG + 5439.268 - 11.736 * T$
	${}^0L_{HgIn}^{FCC\_A1} = -20922.892 + 90.228 * T$
	${}^1L_{HgIn}^{FCC\_A1} = 178.385 + 68.866 * T$
Tetragonal_A6	${}^0L_{HgIn}^{Tetragonal\_A6} = 11507.390 + 6.134 * T$
	${}^1L_{HgIn}^{Tetragonal\_A6} = 25000.000$
GHSERHG	200.00 < T < 234.32: 82,356.855 − 3348.19466*T + 618.193308*T*LN(T) −2.0282337*T**2 + 0.00118398213*T**3 − 2366,612*T**(−1) 234.32 < T < 400.00: −8961.207 + 135.232291*T − 32.257*T*LN(T) +0.0097977*T**2 − 3.20695E − 06*T**3 + 6670*T**(−1) 400.00 < T < 700.00: −7970.627 + 112.33345*T − 28.414*T*LN(T) +0.00318535*T**2 − 1.077802E − 06*T**3 − 41,095*T**(−1) 700.00 < T < 2000.00: −7161.338 + 90.797305*T − 24.87*T*LN(T) − 0.00166775*T**2 +8.737E − 09*T**3 − 27,495*T**(−1)
GHSERIN	200 < T < 429.75: −6978.89 + 92.338115*T − 21.8386*T*LN(T) −0.00572566*T**2 − 2.120321E − 06*T**3 − 22,906*T**(−1) 429.75 < T < 3800.00: −7033.516 + 124.476588*T − 27.4562*T*LN(T) +5.4607E − 04*T**2 − 8.367E − 08*T**3 −211,708*T**(−1) + 3.53116E + 22*T**(−9)
GFCCIN	200.00 < T < 429.75: −6816.829 + 92.338115*T − 21.8386*T*LN(T) −0.00572566*T**2 − 2.120321E − 06*T**3 − 22,906*T**(−1) 429.75 < T < 3800.00: −6871.455 + 124.476588*T − 27.4562*T*LN(T) +5.4607E − 04*T**2 − 8.367E − 08*T**3 −211,708*T**(−1) + 3.53116E + 22*T**(−9)

GFCCIN: Gibbs free energy of In in FCC_A1 structure.

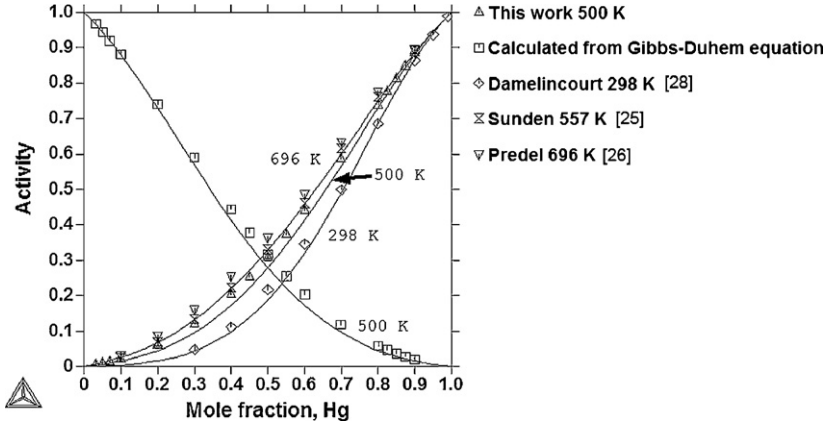

Fig. 3. Calculated activities of mercury and indium at 500 K and mercury at 298 K superimposed with experimental points.

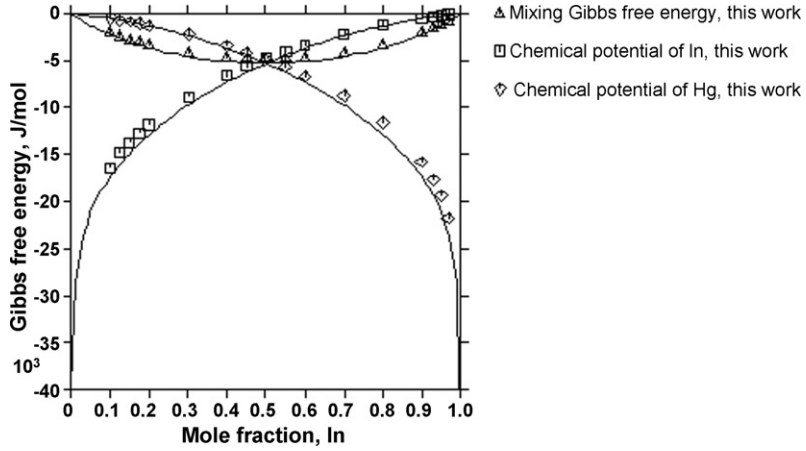

Fig. 4. Calculated Gibbs energy of mixing and chemical potentials of mercury and indium at 500 K superimposed with experimental points.

imposed with experimental points is shown in Fig. 5. Difference between calculated line and experimental data of Kleppa [20,21] and Bros [23] is less than 200 J/mol, which is comparable with the uncertainty of experimental enthalpy data. One can find from the figure, that enthalpy of mixing was not dependent on temperature and used model describes the heat of mixing well.

Fig. 6 shows the calculated phase diagram compared with experimental data. Generally, calculated phase diagram is in good agreement with the experimental data. The only difference between calculated and measured liquidus line is seen around the composition of HgIn intermetallic compound. However, taking into account invariant reactions between HgIn and other phases, one cay say that IMC phase is modeled well. Liquidus line on indium side is reproduced well and agrees with experimental data obtained by several authors.

Detailed information about calculated invariant reactions is collected in Table 4. In the same table literature information about invariant reaction is gathered. The comparison of calculated and measured values suggests good agreement between experiments

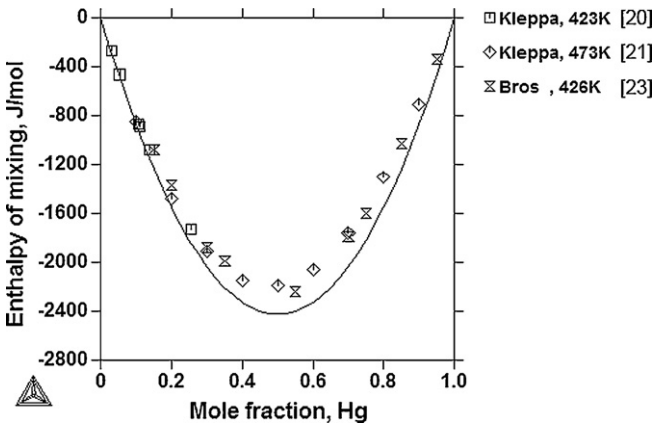

Fig. 5. Calculated enthalpy of mixing of the liquid phase.

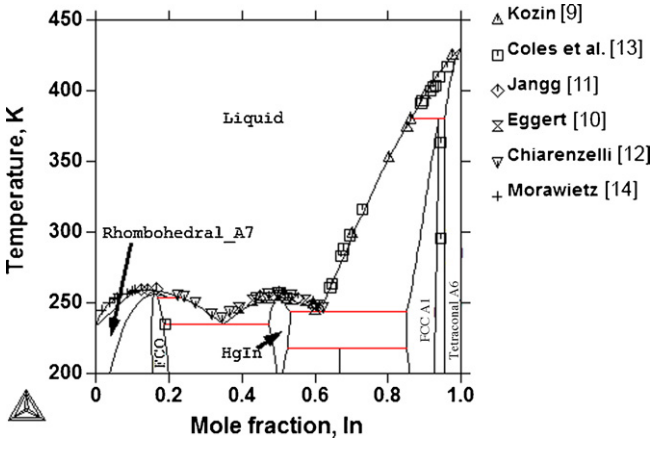

Fig. 6. Calculated phase diagram of Hg–In system superimposed with experimental points.

Table 4
Invariant reactions.

Reaction	Experiment			Calculation	
	X (In)	T [K]	Lit.	X (In)	T [K]
L + Rhombo ⇔ FCO	≈0.16	253	[21]	0.168	253.6
L ⇔ FCO + HgIn	0.34	236	[21]	0.346	235.6
HgIn + FCC_A1 ⇔ $HgIn_2$	0.667	218	[21]	0.667	218
L ⇔ HgIn + FCC_A1	0.61	243	[21]	0.61	243.7
L + Tetra ⇔ FCC_A1	0.939	381	[21]	0.938	380.8
L ⇔ Rhombo	0.14	236	[21]	0.138	235.6
L ⇔ HgIn	0.5	254	[21]	0.5	252.6

and calculation. As compared with previous assessment done by Hansen [41] we obtained the same agreement with experimental description of the phase diagram. The biggest difference is that we used different reference state which allows to expand the description to high-ordered systems without additional calculations. Calculated activity of mercury based on our approach is in better agreement with experimental data than Hansen's [41] proposition and shows very good reproduction of Damelincourt et al. [28] data. Opposite to Hansen [41], we did not use Okajima and Sako's [27] data because the experimental points show unexpected, constant values for concentration between 0.3 and 0.4 mole fraction of In. Calculated enthalpy of mixing shows slightly lower values than measured one. However, the same situation one can find in Hansen's work. Generally, our assessment shows the same reproduction of the phase diagram and enthalpy of mixing as Hansen's [41] work, and better agreement with experimental information about activities.

7. Conclusions

The activities of Hg in the binary Hg–In system were experimentally determined by vapor pressure method at 460–940 K. The activities show negative deviation form the Raoult's Law. Using the experimental results of this study and literature information, the thermodynamic model of the Hg–In systems was re-optimized and a new set of interaction parameters was found. It was found that the calculated thermodynamic properties and phase diagram are in good agreement with the experimental data.

Acknowledgment

W. Gierlotka and S.-W. Chen are thankful to National Science Council of Taiwan for the financial support (NSC 96-2221-E-007-001).

References

[1] R. Corsini, A.D. Bortolozo, M.S. da Luz, R. Ricardo da Silva, C.A.M. dos Santos, A.J.S. Machado, Mater. Lett. 61 (1) (2007) 263–266.
[2] V. Leute, H.M. Schmidtke, J. Phys. Chem. Solids 49 (1988) 1317–1325.
[3] M.F. Merriam, M.A. Jensen, B.R. Coles, Phys. Rev. 130 (1963) 1719–1726.
[4] H. Ito, E. Ogawa, T. Yanagase, Nippon Kinzoku Gakkai-Shi 15 (1951) 382–384.
[5] W.M. Spicer, C.J. Banick, J. Am. Chem. Soc. 75 (1953) 2268–2269.
[6] C. Tyzack, G.V. Raynor, Trans. Faraday Soc. 50 (1954) 675–684.
[7] L.F. Kozin, P.S. Niegmetova, M.B. Dergacheva, Termodinamika binarnych amalgamnych system, Nauka, Alma-Ata, 1977.
[8] T.X. Mahy, B.C. Gissen, J. Less-Common Metals 63 (1979) 257–264.
[9] L.F. Kozin, N.N. Tananaeva, Zh. Neorg. Khim. 6 (1961) 463–465.
[10] G.L. Eggert, Trans. ASM 55 (1962) 891–897.
[11] G. Jangg, Z. Metallkde 53 (1962) 612–614.
[12] R.V. Chiarenzelli, O.L.I. Brown, J. Chem. Eng. Data 7 (1962) 477–478.
[13] B.R. Coels, M.F. Merriam, Z. Fisk, J. Less-Common Metals 5 (1963) 41–48.
[14] W. Morawietz, Chemie-Ing. Technol. 36 (1964) 638–647.
[15] T. Claeson, M.F. Merriam, J. Less-Common Metals 11 (1966) 186–190.
[16] T.B. Massalski, J.L. Murray, L.H. Bennet, H. Baker, in: T.B. Massalski (Ed.), Binary Alloy Phase Diagrams, American Society for Metals, Metals Park, OH, 1986, p. 1326.
[17] W. Heller, L.E. Musgrave, J. Less-Common Metals 20 (1970) 77–82.
[18] T.W. Richards, J.H. Wilson, Z. Phys. Chem. 72 (1910) 129–164.
[19] J.N. Butler, J. Phys. Chem. 68 (1964) 1828–1833.
[20] O.J. Kleppa, M. Kaplan, J. Phys. Chem. 61 (1957) 1120–1123.
[21] O.J. Kleppa, Acta Metall. 8 (1960) 435–445.
[22] F.E. Witting, P. Scheidt, Naturwissenschaften 47 (1960) 250–251.
[23] J.P. Bros, Compt. Rend. 260 (1965) 3935–3938.
[24] H.P. Singh, S. Misra, J. Less-Common Metals 32 (1973) 227–235.
[25] N. Sunden, Z. Elektrochem. 57 (1953) 100–102.
[26] B. Predel, D. Rothacker, Acta Metall. 15 (1967) 135–141.
[27] K. Okajima, H. Sako, Trans. Jpn. Inst. Metals 32 (1973) 227–580.
[28] B. Damelincourt, J.J. Desbaratas, J. Villan, P. Waguet, Compt. Rend. B 270 (1970) 1661–1664.
[29] U.R. Kattner, J. Miner. Metals Min. Soc. 49 (12) (1997) 14–19.
[30] W. Gibson, Proc. Roy. Soc., Edin. 23 (1912) 1–12.
[31] C.G. Jackson, J. Chem. Soc. 99 (1911) 1006–1012.
[32] W. Ptak, M. Sukiennik, Bull. Acad. Polish Sci. Technol. 23 (1975) 687–691.
[33] M. Fik, M. Kucharski, W. Ptak, M. Sukiennik, Arch. Hutn. 1 (1976) 157–160.
[34] W. Gierlotka, K. Fitzner, M. Sukiennik, J. Miner. Metals, 38 (3–4) B (2002) 237–243.
[35] S. Malecki, PhD Thesis, AGH Univ. Sci. Technol., 1992.
[36] Statgraphics 5.0, StatPoint, Inc. 2325 Dulles Corner Boulevard, Suite 500, Herndon, Virginia 20171, USA.
[37] ThermoCalc v. R. Foundation Computational Thermodynamic, Stockholm, Sweden, 2006.
[38] W. Gierlotka, J. Sopousek, K. Fitzner, Calphad 30 (2006) 425–430.
[39] E.A. Guggenheim, Trans. Faraday Soc. 33 (1937) 151–155.
[40] M. Temkin, Acta Phys. Chim. 20 (1945) 411–420.
[41] S.C. Hansen, Calphad 22 (3) (1998) 359–372.
[42] PURE 4.4 SGTE Pure Elements (Unary) Database, Scientific Group Thermodata Europe, 1991–2006.
[43] R. Schmid-Fetzer, D. Andersson, P.Y. Chevalier, L. Eleno, O. Fabrichnaya, U.R. Kattner, B. Sundman, C. Wang, A. Watson, L. Zabdyr, M. Zinkevich, Calphad 31 (2007) 38–52.